이학석사 학위논문

생쥐의 간 허혈-재관류 손상에서 Phosphoinositide 3-Kinase p110γ 의 역할

Deficiency of Phosphoinositide 3-Kinase p110γ Ameliorates Hepatic Ischemia-Reperfusion Injury in Mice

울 산 대 학 교 대 학 원

의 학 과

김 민 경

생쥐의 간 허혈-재관류 손상에서 Phosphoinositide 3-Kinase p110γ 의 역할

지 도 교 수 황 신

지 도 교 수 김 나 영

이 논문을 이학석사학위 논문으로 제출함

2018 년 **12** 월

울 산 대 학 교 대 학 원

의 학 과

김 민 경

김 민 경의 이학석사학위 논문을 인준함

심사위원 정 동 환 (인)

심사위원 황 신 (인)

심사위원 김 나 영 (인)

울 산 대 학 교 대 학 원

2018년 12월

Master of Science

Deficiency of Phosphoinositide 3-Kinase p110γ Ameliorates Hepatic Ischemia-Reperfusion Injury in Mice

The Graduate School

of the University of Ulsan

Department of Medicine

Minkyung Kim

Deficiency of Phosphoinositide 3-Kinase p110γ Ameliorates Hepatic Ischemia-Reperfusion Injury in Mice

Supervisors: Profs. Shin Hwang and

Nayoung Kim

A Dissertation

Submitted to

The Graduate School of the University of Ulsan

In Partial Fulfillment of the Requirements

For the Degree of

Master of Science

by

Minkyung Kim

Department of Medicine

Ulsan, Korea

December, 2018

Contents

그림목차

Abstract

Background: Tissue ischemia-reperfusion injury (IRI) generally occurs when blood supply to an organ or tissue is abruptly interrupted and blood circulation is resumed subsequently, that leads to an acute inflammatory response. Ischemia-reperfusion injury models are often used for the research on the complications of resectional surgery and transplantation. Our previously study shows that the treatment of PI3K p110γ-specific inhibitor can reduce kidney ischemia-reperfusion injury. Therefore, this study was set up to understand the role of PI3K p110γ in liver ischemia-reperfusion injury using PI3K p110γ-deficient ($p110\gamma^{-/-}$) mice.

Methods: Hepatic warm ischemia was performed for 90 minutes by clamping the portal triad and reperfusion was initiated by removal of the clamp. After 3 or 24 hours of reperfusion, the mice were sacrificed. Liver damage was evaluated by serum alanine aminotransferase (ALT) level and tissue histology. The expression of pro-inflammatory cytokines was determined by qPCR as well as by intracellular staining for flow cytometry. Immune cell populations in the liver were determined by flow cytometry.

Results: I found that hepatic IRI was ameliorated in PI3K $p110\gamma^{-/-}$ mice by serum ALT levels

and histopathological analysis. The livers form PI3K p110γ$^{-/-}$ mice had less transcripts of pro-inflammatory cytokines such as interleukin (IL)-6 and IL-17 than those of heterozygous control mice at 3 and 24 hours post-ischemia. The reduction of IL-6 and IL-17 transcripts at 3 hours was statistically significant. The results of flow cytometry show that IL-6 was produced mainly in CD11b^{+} monocytes/macrophages in the insulted liver. In addition, total macrophages in the liver of p110γ$^{-/-}$ mice were reduced after 3 hours of reperfusion. Particularly, CD11b^{+}F4/80^{+} infiltrated macrophages were significantly decreased in the livers from p110γ$^{-/-}$ mice. Nonetheless, The ratio of M1/M2 subsets was not changed.

Conclusion: I found that the genetic deficiency of PI3K p110γ alleviated hepatic IRI in mice. These results suggest that PI3K p110γ$^{-/-}$ mice have decreased expression of inflammatory cytokines in the liver upon LIRI, as a result of the reduced trafficking of macrophages.

Introduction

Interruption of blood flow to an organ or tissue and subsequent reperfusion lead to an acute inflammatory response that may cause significant cellular damage and organ dysfunction. Liver ischemia-reperfusion injury (LIRI) is important in a number of clinical situation, including hepatic resectional surgery and liver transplantation [1-4]. A period of ischemia cannot be avoided during a number of surgical procedures on the liver, especially liver transplantation [5, 6]. On restarting the blood supply, the liver goes through further damage, aggravating the injury already caused by ischemia [7]. In hepatic transplantation, it could cause an array of conditions with clinical outcome of a poorly functioning graft [8]. Mouse model of LIRI can be adopted for the research on liver transplantation. The process of IRI to the liver is associated with many mutually associated factors that lead to hepatic failure. Activation of Kupffer cells (KCs), migration of neutrophils and monocyte/ macrophages, and reactive oxygen species contribute to the pathogenesis of LIRI [9]. The liver has a high content of resident immune cells to maintain the homeostatic state. Particularly, KCs, the resident macrophages found in the liver, might be main responding

cells to IRI. KCs become activated during reperfusion. An inflammatory response by activated KCs is identified as a pivotal mechanism of injury during reperfusion [10-12]. Ischemia itself can activate KCs as well [13]. When activated, they produce pro-inflammatory cytokines, such as interleukin-1 (IL-1), tumor necrosis factor-α (TNF-α), interleukin-6 (IL-6), and interferon-γ (INF-γ) [14]. Liver IRI can be also characterized by the infiltration of large amounts of circulating monocyte-derived macrophages, called infiltrated macrophages [15]. Circulating monocytes are recruited to tissues in homeostasis and injury-associated inflammation. Infiltrated monocyte and its descendants are plastic and can either promote inflammation (M1 macrophage) or assist the healing process (M2 macrophages), depending on the type of injury and the tissue environment [16]. Studies on acute and chronic liver injury, such as acetaminophen-induced liver injury or liver fibrosis, show that infiltrated monocytes contribute to pathogenesis as recruited to the inflamed liver in human and mouse [17-19].

Phosphatidylinositol (3,4,5)-trisphosphate (PIP_3) operates as a second messenger by recruiting pleckstrin homology (PH) domain-containing proteins to the plasma membrane.

They activate signaling pathways that promote proliferation, survival, differentiation, and chemotaxis [20]. Class I phosphatidylinositol-4,5-bisphosphate 3-kinases (PI3Ks) are subdivided into 2 groups based on their structure: Class IA PI3Ks are heterodimers consisting of one regulatory subunit (p85α, p85β, p50α, p55α, or p55γ) and one catalytic subunit (p110α, p110β, or p110δ), whereas class IB PI3Ks are heterodimers consisting of one regulatory subunit (p101 or p84) and a single catalytic subunit (p110γ) [21]. PI3K p110γ is a crucial signaling molecule required for macrophage migration and accumulation in inflammation [22].

In a previously study, our group has shown that PI3K p110γ-specific inhibition ameliorates renal ischemia-reperfusion injury through reducing B and T cell migration to the kidney [23]. In the case of the kidney, there are not many immune cells in the healthy organ. However, liver is an organ of predominant innate immunity, playing an important role not only in host defenses against invading microorganisms and tumor transformation but also in liver injury and repair [24]. In acute inflammation caused by renal ischemia-reperfusion injury, migration of immune cells to the tissue plays an important role, but in the liver, the

role of resident innate immune cells can be important. The innate immune system senses danger signals from damaged hepatocytes during non–infection-related liver injury, resulting in an inflammatory response. This sterile inflammation not only contributes to liver injury but may also be involved in liver repair. For example, acetaminophen hepatotoxicity and LIRI are associated with sterile neutrophilic inflammation, which contributes to liver injury [25, 26]. On the other hand, sterile neutrophilic inflammation after partial hepatectomy could promote liver regeneration by triggering a local inflammatory response and liver myeloid cell-dependent release of TNF-α and IL-6, leading to hepatocyte proliferation [27]. TNF-α, IL-1 and IL-6 are increased during LIRI by activated KCs as well [28]. These previous studies show that the early stages of liver damage accompany with cytokine production, chemokine release, and subsequent infiltration of inflammatory cells into the liver.

Therefore, in order to elucidate the role of PI3K p110γ in LIRI, cytokine gene expression and infiltrated immune cells to the damaged liver were assessed using systematic PI3K p110$\gamma^{-/-}$ mice. This study shows that the deficiency of p110γ reduced IL-6 mRNA and protein in $CD11b^{+}$ monocyte/macrophages and decreased infiltration of monocytes to the

liver, alleviating acute inflammatory injury by liver ischemia-reperfusion.

Materials & Methods

Animals

PI3K p110γ knock-out (KO) (p110γ$^{-/-}$) mice and p110γ$^{+/-}$ or p110γ$^{+/+}$ mice as wild-type (WT) control on a C57BL/6 (B6) background were housed under specific pathogen-free conditions at Laboratory of Animal Research, Disease Animal Resource Center, Asan Medical Center, Seoul, Republic of Korea. PI3K p110γ$^{-/-}$ mice were a kind gift from Prof. E. Hirsch (University of Torino, Italy) [22]. The mice used were sex- and age-matched littermates, between 6 and 14 weeks of age. All procedures were approved by the Institutional Animal Care and Use Committee, Asan Medical Center (IACUC Approval No. 2014-13-006).

Genotyping

Genomic DNA (gDNA) was isolated from mouse tails using gDNA prep kit (BIOFACT, South Korea). gDNA was amplified by polymerase chain reaction (PCR) using C1000 Touch™ Thermal Cycler (Bio-Rad, CA, USA) with following primers: PI3K p110γ

WT, forward, 5'-GGA GAA CTA TGA ACA ACC GG-3'; reverse, 5'-CAA CTT CCA GTA ATG CAG GC-3', and PI3K p110γ KO, forward, 5'- CTG CTC TTT ACT GAA GGC TC-3'; reverse, 5'- CAA CTT CCA GTA ATG CAG GC-3'. PCR thermocycling condition was as follows: 10 cycles for 30 s at 95℃, for 30 seconds at 65℃, and for 30 seconds at 72℃ and 25 cycles for 30 seconds at 94℃, for 30 seconds at 65℃, and for 30 seconds at 72℃. Amplified DNA was separated by 1.5% agarose gel electrophoresis. Expected band sizes were: 373 bp for PI3K p110γ WT; 550 bp for PI3K p110γ KO.

Murine LIRI model

Nonlethal segmental (70%) hepatic warm ischemia was performed for 90 minutes under anesthesia with zoletil/rompun. Liver IRI was performed as described previously with minor modifications [29]. Surgery was initiated with a midline laparotomy. With the use of an operating microscope, the liver hilum was dissected free of surrounding tissue. All structures in the portal triad (hepatic artery, portal vein and bile duct) to the left and median liver lobes were occluded with a microvascular clamp for 90 minutes; reperfusion was

initiated by removal of the clamp. The abdomen was covered with a sterile gauze to minimize dehydration. Mice were kept warm during all the procedures. Sham operation was performed in same way but without clamping.

ALT assay

Whole blood was collected by heart puncture and the serum was prepared by centrifugation at 5000 rpm at 24℃ for 20 minutes, following incubation at 37℃ for 15 minutes. ALT assay was performed by Comparative Pathology Core Facility, Convergence Medicine Research Center, Asan Medical Center.

Histology

Upper 70% lobes of ischemic liver were harvested after brief perfusion with PBS through the portal vein. A middle-sized lobe of the liver was fixed in 4% formalin, embedded in paraffin, sectioned, and stained with hematoxylin-eosin (H&E) following standard protocols. The preparation of the slides were performed by Comparative Pathology Core

Facility, Convergence Medicine Research Center, Asan Medical Center. Acute tissue damage was assessed as a loss of nucleus. Magnification was x40. The damaged region of the liver was quantified by IMT i-solution program (IMT i-solution Inc, Daejeon, Republic of Korea).

Quantitative real-time reverse-transcription PCR (qPCR).

Total RNA was extracted from the liver tissue using the TRIzol reagent (Invitrogen, Carlsbad, CA), and the concentration and purity of RNA were measured using Nanodrop 2000 (Thermo Fisher Scientific, Waltham, MA). Total RNA of 5 μg was used to synthesize cDNA using Oligo(dT)12-18 primer, SuperScript Ⅲ Reverse Transcriptase, 10 mM dNTP Mix, and RNase OUT (all from Invitrogen, Carlsbad, CA). Messenger RNA (mRNA) expression for IL-6, IL-17, and IL-10 was quantified by SYBR Green (Applied Biosystems, Foster City, CA) two-step real-time RT-PCR, using an ABI 7900 Sequence Detection System (Applied Biosystems, Foster City, CA). Each primer sequence is as follows: IL-17 primers, forward, 5'-ATC AGG ACG CGC AAA CAT G-3'; reverse, 5'-TGA TCG CTG CTG CCT TCA C-3' [30], IL-6 primers, forward, 5'-CTG CAA GAG ACT TCC ATC CAG-3'; reverse,

5’-AGT GGT ATA GAC AGG TCT GTT GG-3’ [31], IL-10 primer, forward, 5’-ATT TGA ATT CCC TGG GTG AGA A-3’; reverse, 5’-ACA CCT TGG TCT TGG AGC TTA TTA A-3’ [32], and GAPDH primers, forward, 5’-TTG TCA GCA ATG CAT CCT GCA C-3’; reverse, 5’-ACA GCT TTC CAG AGG GGC CAT C-3’. All reactions were performed in triplicates using thermal cycling conditions as follow; 2 minutes at 50℃, 10 minutes at 95℃ followed by 40 cycles of 95℃, 15 seconds, and 60℃, 1 minute. Ct value was determined by an SDS software v2.4 (Applied Biosystems, Foster City, CA). The expression of each gene was normalized to GAPDH mRNA content and calculated using comparative Ct methods [33].

Liver immune cell isolation

One lobe of the harvested liver was chopped up with scissors and dissociated using GentleMACS dissociator (Miltenyi Biotec, Bergisch Gladbach, Germany) in dissociation buffer (0.5 M $CaCl_2$, 0.2 M $MgCl_2$, 3 mg/ml Collagenase Type IV (Sigma Aldrich, St. Louis, MO), 30,000 U/ml DNase I solution (Roche, Basel, Switzerland), 1x PBS). The cell suspension was filtered with a 100 μm nylon cell strainer (CORNING, Corning, NY) and

centrifuged. To isolate immune cells, the cell pellet was suspended in 36% Percoll and layered onto 72% Percoll gradient (GE Healthcare, Chicago, IL) in a 15 ml conical tube, and centrifuged at 2000 RPM at 24℃ for 30 minutes without brake. Immune cells in the middle layer were collected and washed twice with 1x PBS. Cells were suspended in RPMI 1640 (Welgene, Gyeongsan-si, Gyeongsangbuk-do, Republic of Korea) with 10% FBS (Sigma Aldrich, St. Louis, MO), 55 μM 2- Mercaptoethanol (Gibco , Waltham, MA) 1 mM sodium pyruvate (Sigma Aldrich, St. Louis, MO), 1% Penicillin/streptomycin (CORNING, Corning, NY), and the cell number was counted using a hemocytometer for further experiment.

Flow cytometry

Isolated immune cells as above were prepared at $3x10^5$ cells/tube for surface staining and $1x10^6$ for intracellular staining. Cells were treated with Fc-blocking rat anti-mouse CD16/32 monoclonal antibody (mAb) (clone 2.4G2, BioLegend, San Diego, CA) to prevent nonspecific binding, and stained with fluorescence-conjugated anti-CD11b (clone M1/70), anti-Gr-1 (RB6-8C5), anti-F4/80 (T45-2342), anti-CD45 (30-F11), anti-CD11c

(N418), anti-MHC class II (M5/114.15.2), and/or anti-Ly6C (HK1.4) monoclonal antibodies (mAbs) at 4℃ for 30 minutes. All the mAbs and their adequate isotype controls were purchased from BioLegend (San Diego, CA, USA) or BD Biosciences (Franklin Lakes, NJ. USA). Cells were fixed with 4% Paraformaldehyde at room temperature for 30 minutes. For intracellular staining, cells were fixed, and permeabilized using Fixation/Permeabilization kit (BD Biosciences, Franklin Lakes, NJ) according to the manufacturer's protocol, followed by incubation with V450-conjugated anti-IL-6 (clone MP5-20F3) and anti-IL-17 (clone TC11-18H10) mAbs from BD Biosciences (Franklin Lakes, NJ). For IL-17 intracellular staining, cells were stimulated with 50 ng/ml PMA and 1 μg/ml Ionomycin (both from Sigma-Aldrich. MO, USA) in the presence of brefeldin A (Thermo Fisher Scientific, Waltham, MA) in 37℃, 5% CO_2 incubator for 5 hours. Flow Cytometric analysis was performed with a FACS Canto II flow cytometer (BD Biosciences, Franklin Lakes, NJ) or a CytoFlex flow cytometer (Beckman Coulter, Brea, CA) and analyzed with a FlowJo V10 software (FlowJo, LLC., Ashland, OR). FACS Canto II was operated by Flow cytometry Core Facility, Research Development Support Center, Asan Medical Center. Absolute cell numbers for each

subpopulation were calculated by multiplying the percentage of each population by the weight of the livers.

Statistical analysis

Student *t*-test, and standard deviations (SD) were calculated by MS EXCEL (Microsoft Corporation, Redmond, WA). Unpaired, two-tailed *t* test and calculation of the standard error of the mean (SEM) were performed with GraphPad Prism 4 (GraphPad, San Diego, CA). *P<0.05; **P<0.01; ***P<0.001.

Result

Deficiency of PI3K p110γ reduced liver damage following LIRI in mice.

To determine the role of PI3K p110γ in hepatic IRI, the warm IR procedure was conducted in WT (p110γ$^{+/-}$ or p110γ$^{+/+}$) and PI3K p110γ$^{-/-}$ mice. The severities of LIRI was accessed by serum ALT concentrations at 3 hours and 24 hours of reperfusion. ALT levels represent the degree of liver damage following LIRI. Serum ALT levels were significantly lower in PI3K p110γ$^{-/-}$ than those of WT mice at 3 hours and 24 hours of reperfusion (Fig. 1A). Compared with those of WT, serum ALT levels were decreased in PI3K p110γ$^{-/-}$ mice by 49.33% and 86.80% at 3 and 24 hours of reperfusion, respectively (Fig. 1A). These data were consistent with the histological alterations in the liver tissues. The liver tissues from WT mice showed marked damages in morphology at 3 hours and 24 hours of reperfusion, while the damages were significantly reduced in PI3K p110γ$^{-/-}$ mice (Fig. 1B, C).

Figure 1

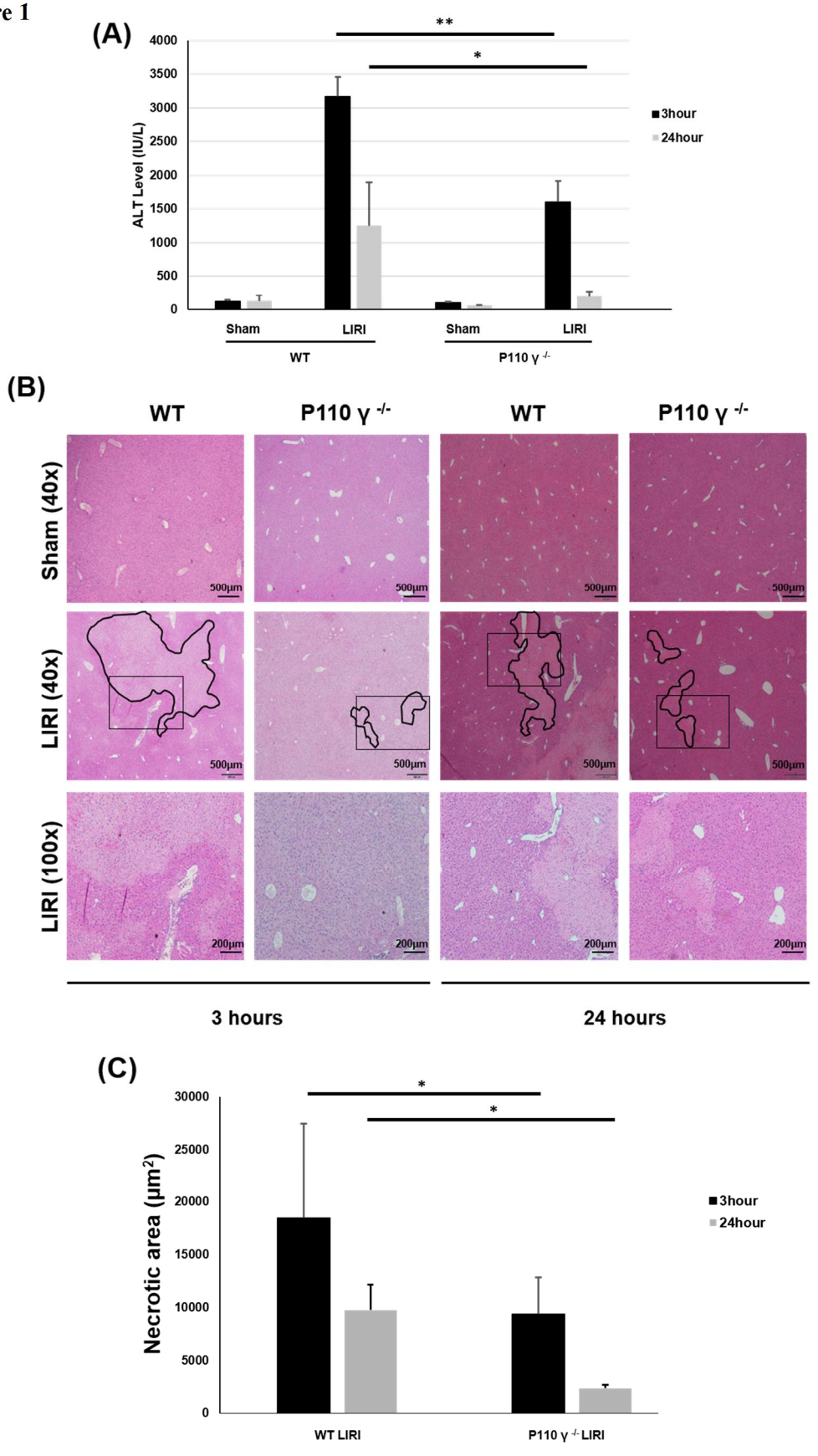
(A)
**
*
ALT Level (IU/L)
4000
3500
3000
2500
2000
1500
1000
500
0
3hour
24hour
Sham
LIRI
Sham
LIRI
WT
P110 γ -/-
(B)
WT
P110 γ -/-
WT
P110 γ -/-
Sham (40x)
LIRI (40x)
LIRI (100x)
500μm
200μm
3 hours
24 hours
(C)
*
*
Necrotic area (μm2)
30000
25000
20000
15000
10000
5000
0
3hour
24hour
WT LIRI
P110 γ -/- LIRI

Figure 1. PI3K p110γ deficiency reduced serum ALT levels and necrosis in the liver in LIRI. (A) Serum ALT was reduced in p110$\gamma^{-/-}$ mice which underwent LIRI. Means + SEM are presented. Student t test was performed. In case of 3 hours' reperfusion: N=6 for WT sham; 14 for WT LIRI; 6 for PI3K p110$\gamma^{-/-}$ sham; 17 for PI3K p110$\gamma^{-/-}$ LIRI. In case of 24 hours' reperfusion: N=2 for WT sham; 4 for WT LIRI; 2 for PI3K p110$\gamma^{-/-}$ sham; 6 for PI3K p110$\gamma^{-/-}$ LIRI. (B) Representative histological results are shown as H & E-stained liver sections from WT and PI3K p110$\gamma^{-/-}$ mice following ischemia for 90 minutes and reperfusion for 3 or 24 hours. The closed fields in the middle row represent necrotic area. The inset boxes are further magnified to x100 in the lower row. (C) The necrotic areas were evaluated with an i-solution program. The graphs indicate the area of three randomly chosen microscopic fields. N= 3 for 3 hours' reperfusion, 1 for 24 hours' reperfusion. Means + SEM are displayed. Student t test was performed. * $P < 0.05$, **$P < 0.01$.

Transcripts of pro-inflammatory cytokines were significantly decreased in the liver of p110γ$^{-/-}$ mice.

Real time qPCR analysis was performed to assess the expression of inflammatory cytokines in the liver. The expression levels of IL-6 and IL-17 were prominently increased after LIRI in WT mice, compared with those of sham. The expression of IL-6 and IL-17 was decreased in the liver from p110γ$^{-/-}$ mice following LIRI by 84.23% and 82.98% in 3 hours of reperfusion, respectively, compared with those of WT. The reductions were statistically significant. Slight reductions were seen in 24 hours of reperfusion as well. The expression of IL-10, an anti-inflammatory cytokine, was not changed (Fig 2). I also analyzed the transcription of IL-1β and TNF-α, but they did not change in 3 hours of reperfusion either (Data not shown). These findings suggest that p110γ deficiency impaired the expression of inflammatory cytokines which contribute to the pathogenesis of LIRI.

Figure 2

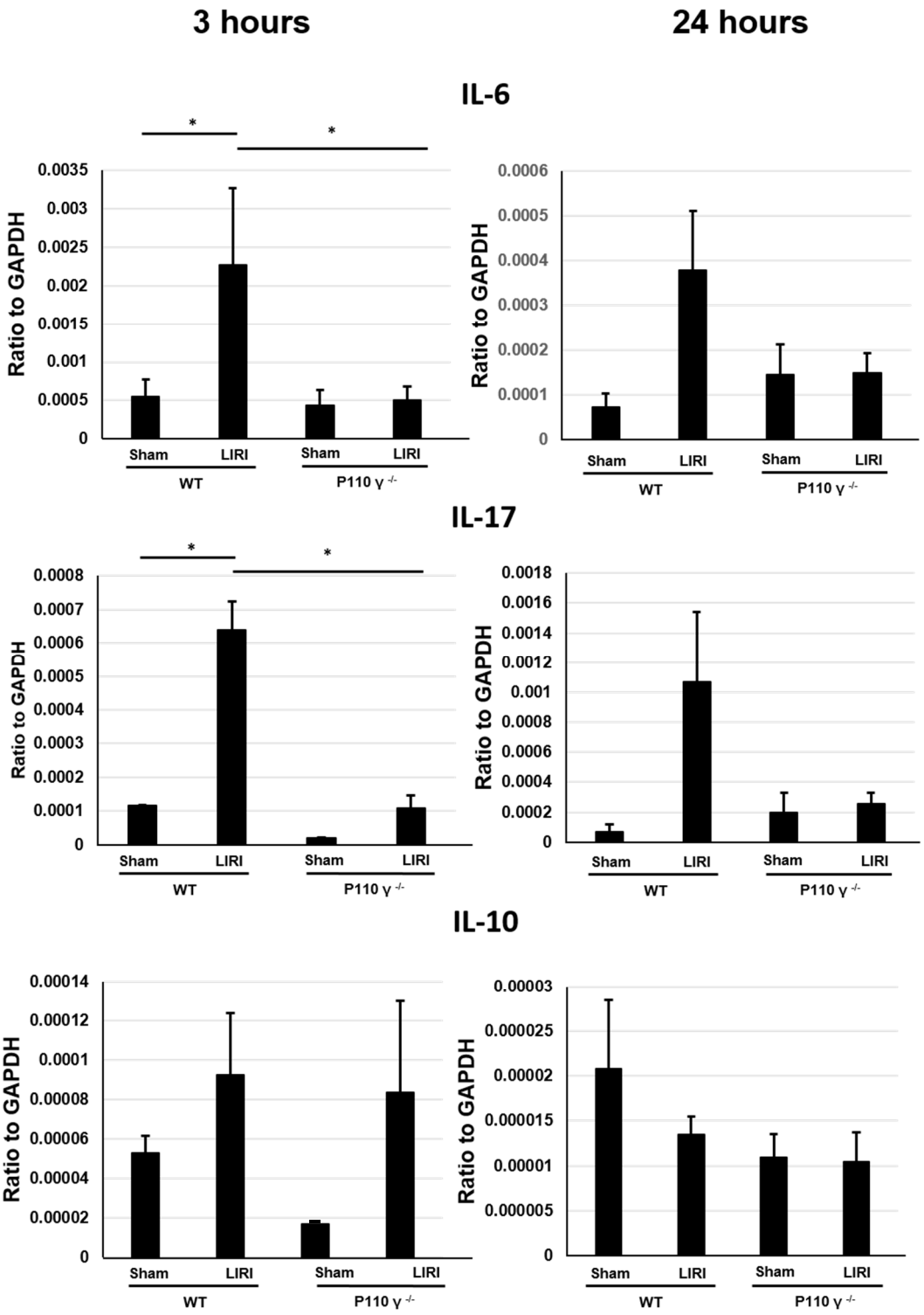
3 hours
24 hours
IL-6
IL-17
IL-10
Ratio to GAPDH
Sham
LIRI
WT
P110 γ -/-
*

Figure 2. Expression of inflammatory cytokines was affected by PI3K p110γ deficiency.

The mRNA expression of inflammatory cytokines was analyzed by qPCR with the livers that were subject to 90 minutes' ischemia and 3 hours or 24 hours of reperfusion. Each value was normalized to the expression of a house-keeping gene, GAPDH. The data represent mean + SEM. In case of 3 hours' reperfusion: IL-6: N= 7 for WT sham; 9 for WT LIRI; 8 for PI3K p110$\gamma^{-/-}$ sham; 8 for PI3K p110$\gamma^{-/-}$ LIRI. For IL-17: N= 6 for WT sham; 3 for WT LIRI; 6 for PI3K p110$\gamma^{-/-}$ sham; 3 for PI3K p110$\gamma^{-/-}$ LIRI. For IL-10: N= 3 for WT sham; 3 for WT LIRI; 3 for PI3K p110$\gamma^{-/-}$ sham; 4 for PI3K p110$\gamma^{-/-}$ LIRI. In case of 24 hours' reperfusion: IL-6: N= 5 for WT sham; 5 for WT LIRI; 5 for PI3K p110$\gamma^{-/-}$ sham; 5 for PI3K p110$\gamma^{-/-}$ LIRI. For IL-17: N= 5 for WT sham; 5 for WT LIRI; 5 for PI3K p110$\gamma^{-/-}$ sham; 5 for PI3K p110$\gamma^{-/-}$ LIRI. For IL-10: N= 5 for WT sham; 5 for WT LIRI; 5 for PI3K p110$\gamma^{-/-}$ sham; 5 for PI3K p110$\gamma^{-/-}$ LIRI. Student t test was performed. * $P < 0.05$, **$P < 0.01$, *** $P < 0.001$.

IL-6 and IL-17 were reduced in p110$\gamma^{-/-}$ mice following LIRI

Flow cytometry was performed to determine which cell type(s) produced IL-6 and IL-17. Cells were isolated from the liver following ischemia for 90 minutes and reperfusion for 3 or 24 hours. The gating strategy is seen in Fig 3A. $CD3^+$ cells are T cells, and $CD11b^+$ cells are mostly monocytes/macrophages. As shown in Fig 3B, IL-6^+ cells were not increased among $CD3^+$ cells at 3 hours of reperfusion, but increased robustly among $CD11b^+$ cells in the liver from WT mice at 3 and 24 hours of reperfusion. IL-6^+ $CD11b^+$ cells were reduced by approximately 50 % in PI3K p110$\gamma^{-/-}$ mice following LIRI, compared with those of WT. $CD11c^+$ dendritic cells and Gr-1^+ neutrophils expressed much less IL-6 than $CD11b^+$ monocytes/macrophages (Data not shown). IL-17 was also reduced in PI3K p110$\gamma^{-/-}$ mice at 24 hours of reperfusion and produced by $CD3^+$ T cells (Fig 3D).

Figure 3

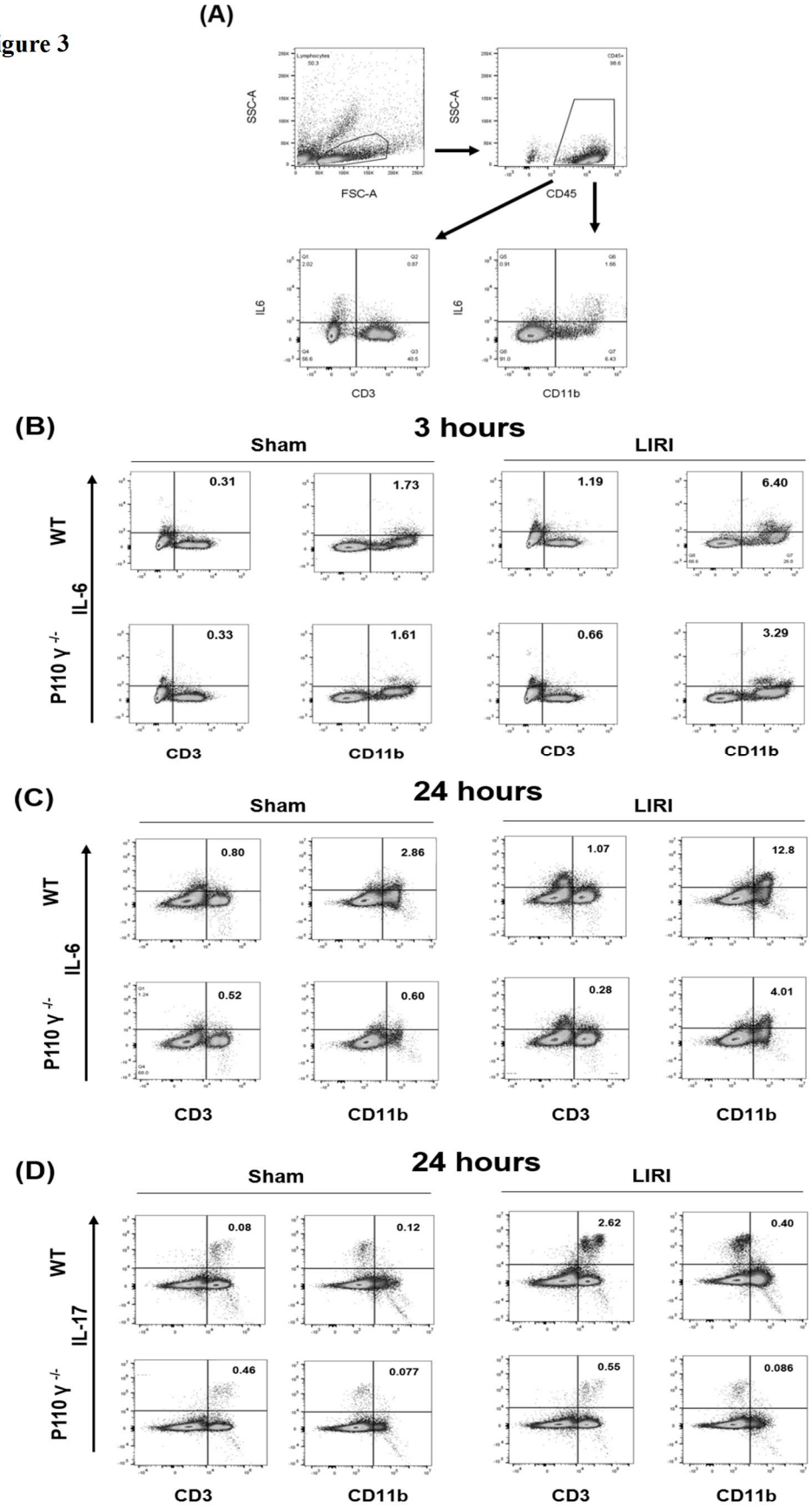
(A)
SSC-A
FSC-A
CD45
IL6
CD3
CD11b
(B)
3 hours
Sham
LIRI
WT
P110 γ -/-
IL-6
0.31
1.73
1.19
6.40
0.33
1.61
0.66
3.29
CD3
CD11b
(C)
24 hours
0.80
2.86
1.07
12.8
0.52
0.60
0.28
4.01
(D)
IL-17
0.08
0.12
2.62
0.40
0.46
0.077
0.55
0.086

Figure 3. IL-6 was produced by macrophages of the liver following LIRI. Liver immune cells were isolated from WT and PI3K p110$\gamma^{-/-}$ mice following sham operation or LIRI. To detect cytokines, intracellular staining was performed for flow cytometry. (A) Gating strategy is shown. Live cells were gated by SSC/FSC and immune cells were defined as $CD45^{+}$. IL-6^{+} cells were analyzed in $CD3^{+}$ T cells and $CD11b^{+}$ macrophages. (B) Representative flow cytometric plots are shown from 3 independent experiments after 3 hours reperfusion. (C,D) Representative plots for IL-6 (C) and IL-17 (D) are shown as above after 24 hours' reperfusion.

PI3K p110γ is responsible for monocyte/macrophage migration to the insulted liver

To identify the role of PI3K p110γ in monocytes/macrophages after liver IRI, the subsets of the liver monocytes/macrophages were analyzed by flow cytometry. $F4/80^+$ macrophages are subdivided into $CD11b^+$ infiltrated macrophages and $CD11b^-$ liver resident macrophages, called Kupffer cells (KCs) [34]. Accordingly, $F4/80^+$ $CD11b^+$ cells were defined as infiltrated macrophages, and $F4/80^+$ $CD11b^-$ cells as KCs (Fig 4A). The percentages and actual cell numbers of total $F4/80^+$ macrophages were significantly reduced in the livers from PI3K $p110\gamma^{-/-}$ mice (Fig 4B). In particular, the percentages and cell numbers of infiltrated macrophages ($CD11b^+$ $F4/80^+$) were decreased in PI3K $p110\gamma^{-/-}$, compared with those of WT mice, after reperfusion of 3 hours (Fig 4C), while Kupffer cell population ($CD11b^-F4/80^+$) was not significantly changed (Fig 4D). These results suggest that infiltrated macrophages could be the key player in reduction of LIRI by PI3K p110γ deficiency.

PI3K p110γ inhibition switches the activation of macrophages form an immunosuppressive M2-like phenotype to a more inflammatory M1-like state [35].

Therefore, I further investigated the effect of PI3K p110γ deficiency on macrophage polarization. Total macrophages were gated from the whole liver immune cells and they were subdivided into M1 and M2 phenotypes (Fig 5A). M1 macrophages are defined as $Ly6C^{low}$ MHC class II^{high}, while M2 are $Ly6C^{low}$ MHC class II^{low} [35]. These results showed that Gr-1 $(Ly6C/G)^{low}$ MHC II^{high} M1 and Gr-1 $(Ly6C/G)^{low}$ MHC II^{low} M2 phenotypes were not significantly changed in WT and PI3K $p110\gamma^{-/-}$ mice following LIRI (Fig 5B, C), although the percentages of M2 macrophages were slightly increased in PI3K $p110\gamma^{-/-}$ mice. Taken together, the results indicate that PI3K p110γ contribute to the infiltration of monocytes/macrophages to the injured liver after LIRI without affecting M1/M2 phenotypes.

Figure 4.

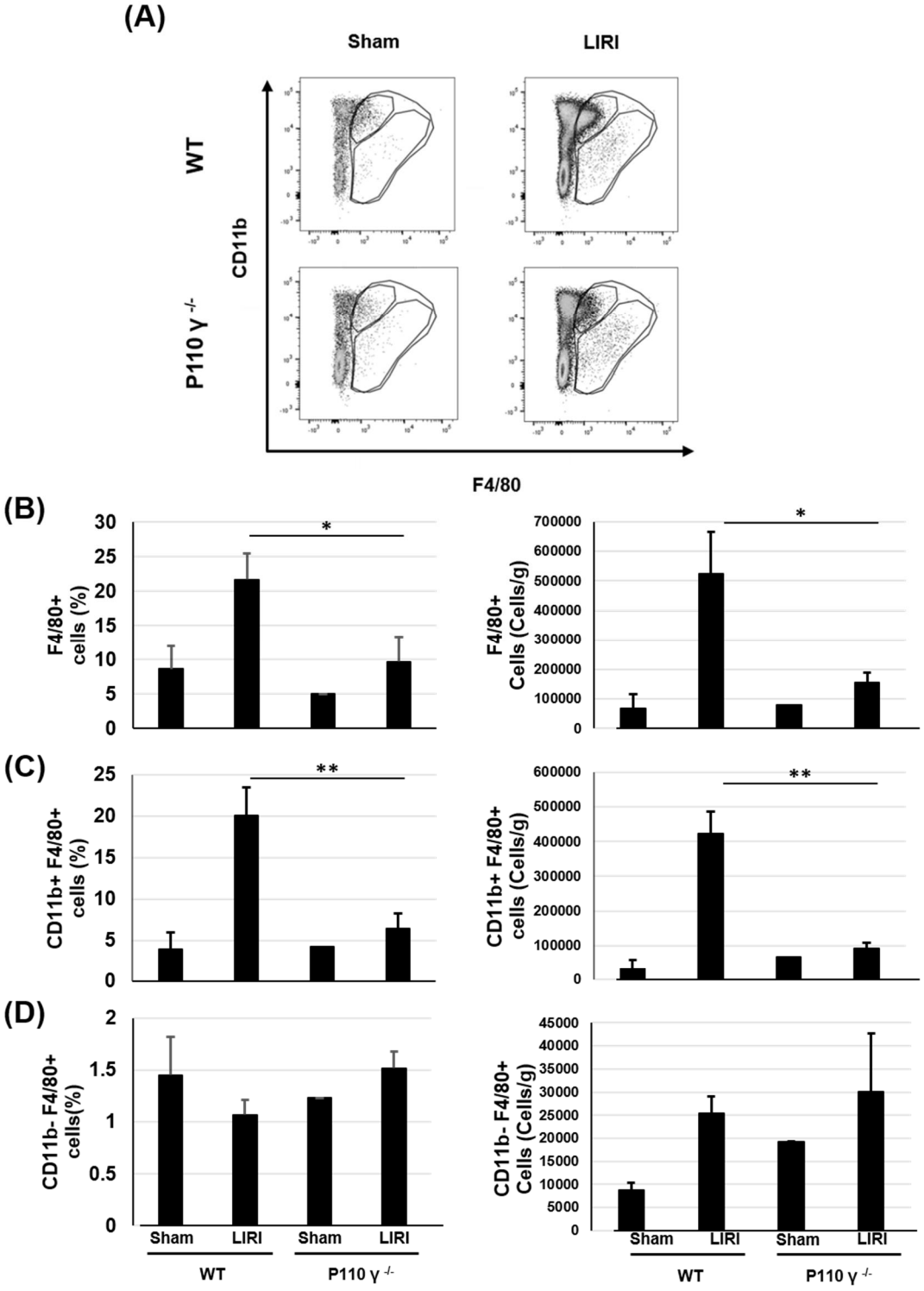
(A)
Sham
LIRI
WT
P110 γ -/-
CD11b
F4/80
(B)
F4/80+ cells (%)
F4/80+ Cells (Cells/g)
(C)
CD11b+ F4/80+ cells (%)
CD11b+ F4/80+ cells (Cells/g)
(D)
CD11b- F4/80+ cells(%)
CD11b- F4/80+ Cells (Cells/g)
Sham
LIRI
WT
P110 γ -/-

Figure 4. Macrophage infiltration to the damaged liver was reduced in PI3K p110γ-/- mice following LIRI. After ischemia for 90 minutes and subsequent reperfusion for 3 hours, the composition of liver immune cells was evaluated by flow cytometry. (A) Representative flow cytometric plots are shown. (B) The values indicate mean+SEM of the percentages (left panel) and the cell numbers (right panel) of $F4/80^+$ cells (total macrophages) out of $CD45^+$ total liver immune cells. (C) The values indicate mean+SEM of the percentages (left panel) and the cell numbers (right panel) of $CD11b^+F4/80^+$ infiltrated macrophages out of $CD45^+$ total liver immune cells. (D) The values indicate mean+SEM of the percentages (left panel) and the cell numbers (right panel) of $CD11b^-F4/80^+$ Kupffer cells out of $CD45^+$ total liver immune cells. Cell numbers were calculated by multiplying the percentages by the liver weight. Student t test was performed. *$P < 0.05$; ** $P < 0.01$. N= 2 for WT sham, 6 for WT LIRI, 1 for PI3K $p110\gamma^{-/-}$sham, 7 for PI3K $p110\gamma^{-/-}$ LIRI.

Figure 5.

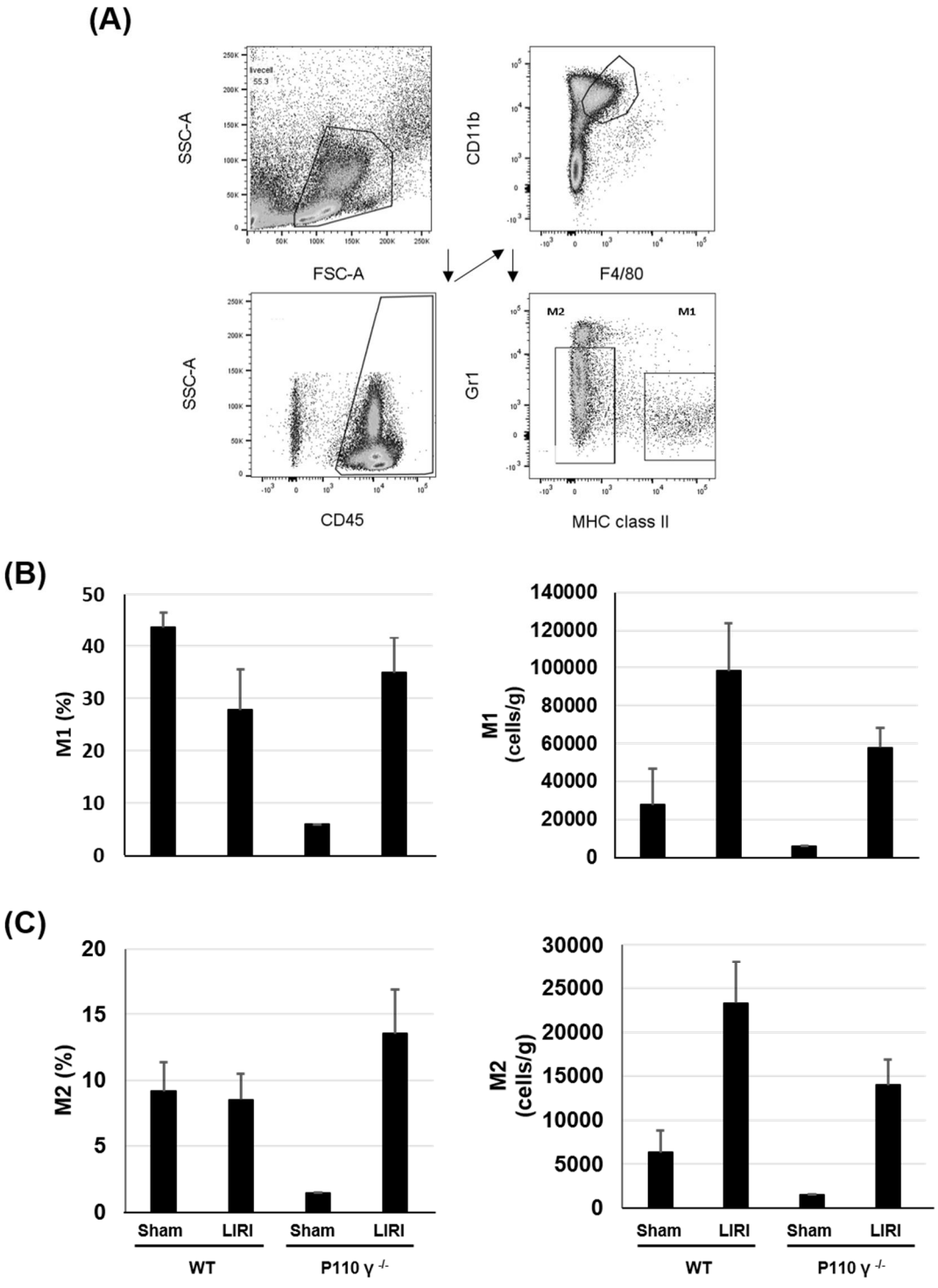
(A)
SSC-A
FSC-A
CD11b
F4/80
SSC-A
CD45
Gr1
MHC class II
M2
M1
(B)
M1 (%)
M1 (cells/g)
(C)
M2 (%)
M2 (cells/g)
Sham
LIRI
Sham
LIRI
WT
P110 γ -/-

Figure 5. PI3Kγ did not contribute to the polarization of macrophages in the liver. (A) Gating strategy is shown to subdivide macrophages into M1 and M2. M1 was defined as MHC class II^{high} $Gr\text{-}1^{low}$ and M2 was defined as MHC class II^{low} $Gr\text{-}1^{low}$. (B) The values represent the means+SEM of the percentages (left panel) and the cell numbers (right panel) of M1 macrophages. (C) The values represent the means+SEM of the percentages (left panel) and the cell numbers (right panel) of M2 macrophages. The percentage of each M1 and M2 was calculated from total macrophages ($F4/80^{+}$). Cell number was calculated as above. N= 2 for WT sham, 7 for WT LIRI, 1 for PI3K $p110\gamma^{-/-}$ sham, and 7 for PI3K $p110\gamma^{-/-}$ LIRI.

Discussion

In this thesis, I demonstrate a role of PI3K p110γ in acute inflammation in the liver using a murine LIRI model for the first time. PI3K p110γ deficiency reduced LIRI through inhibiting the infiltration of monocytes/macrophages into the insulted liver. Macrophages were a main producer of IL-6, which was also down-regulated by PI3K p110γ deficiency. IL-17 was also decreased in the liver of PI3K p110$\gamma^{-/-}$ mice.

Sterile inflammation is marked by the recruitment of neutrophils and macrophages [36]. In murine renal IRI models, PI3K p110γ plays a role in the migration of neutrophils and B cells [23, 37]. PI3K p110γ transmits signals downstream of G protein-coupled receptors (GPCRs), which include chemokine receptors, whereas p110δ is involved in the chemotaxis of B and natural killer (NK) cells [38-40]. The specific role of the PI3K isoform in immune cell migration depends on cell type, target organ, medical condition, and timing. LIRI is also characterized by the infiltration of large amounts of circulating monocyte-derived macrophages [34]. Following liver inflammation, the pool of hepatic macrophages is rapidly expanded by the infiltration of bone marrow-derived monocytes, which become monocyte-

derived macrophages in mice [41]. This study shows that total macrophage population was decreased in PI3K p110$\gamma^{-/-}$ mice following LIRI, compared with WT. Especially, $CD11b^{+}F4/80^{+}$ infiltrated monocyte-derived macrophages were significantly decreased, suggesting a role of PI3K p110γ in monocyte/macrophage migration upon liver damage. PI3K p110γ is needed for optimal migration of macrophages to respond to chemokines, such as monocyte chemotactic protein-1 (MCP-1/CCL2) and colony stimulating factor-1 (CSF-1) *in vitro* [42]. Peritoneal PI3K p110$\gamma^{-/-}$ macrophages show a reduced migration toward a wide range of chemotactic stimuli and a severely defective accumulation in a septic peritonitis model [22]. Taken together, these results demonstrate that PI3K p110γ is a crucial signaling molecule required for macrophage accumulation in various inflammation models of mouse.

Nonetheless, liver is a unique organ which has a high content of resident macrophages, called KCs, in homeostatic state. KCs have been assumed to be the major responding cells against IR, but tissue-resident macrophages clear apoptotic cells to maintain self-tolerance [43], implying a protective role in inflammation. Hence, infiltrated macrophages were suggested to participate in liver injury following LIRI. The difference

between KCs and infiltrated macrophage is noticeable from the developmental stage. As KCs is originated from fetal liver-derived erythromyeloid progenitors, mouse KCs are characterized by $CD11b^{-}F4/80^{+}$ [44, 45]. KC population did not change in this study, although total macrophages were decreased. It demonstrates that the reduction of total macrophages was caused by the decrease of infiltrated macrophages, not KCs.

A macrophage can be polarized to M1 or M2 phenotype, where they express different functional programs in response to microenvironmental signals [46]. M1 macrophages produce proinflammatory cytokines, co-stimulatory molecules including CD80 and CD86, and effector enzymes; M2 produce anti-inflammatory cytokines, immunosuppressive arginase, and scavenger receptors [47]. The role of PI3K p110γ is well described as a molecular switch between immune stimulation and suppression in cancer models [35, 48]. PI3K p110γ signaling in macrophages inhibits NFκB activation but stimulates C/EBPβ activation, thereby promoting immune suppression [48]. The lack of PI3K p110γ induces M1 polarization in acute and chronic kidney diseases in mice, and fails to prevent the progression of kidney diseases [49]. By contrast, PI3K p110γ did not

contribute to the polarization of macrophages in a mouse model of LIRI, although LIRI was significantly reduced in PI3K p110$\gamma^{-/-}$ mice in this study. The underlying mechanism of this discrepancy awaits further investigation, but the tissue-resident macrophages, or lack of them, and/or developmental defect in monocytes/macrophages might have a role in it.

Inflammatory cytokines such as IL-1β, IL-6, TNF-α and IL-17 play an important role in initiating the inflammatory response as well as in pathogenesis. I initially assessed expression of IL-1β, IL-6, TNF-α, IL-17 and IL-10 by qPCR (Data not shown) and found that only IL-6 and IL-17 mRNA were decreased in the liver from PI3K p110$\gamma^{-/-}$ mice following LIRI, compared with those of WT. The role of IL-6 is well known in various inflammatory and autoimmune diseases, in particular, rheumatoid arthritis [50]. Temporally distinct systemic elevations in IL-6 is revealed during LIRI in rats [51]. At 3 hours of reperfusion, majority of IL-6^{+} cells were Gr-1^{-}CD11b^{+}, while Gr-1^{+}CD11b^{+} cells were majority at 24 hours of reperfusion (Data not shown). Gr-1^{+}CD11^{+} cells could be myeloid-derived suppressor cells (MDSC) [52]. IL-6 was produced by CD11b^{+}F4/80^{+} infiltrated macrophages at 3 hours of reperfusion. In this context, the cell type(s) responsible for IL-6

production appears to be changeable upon the time of reperfusion. Many studies demonstrate that IL-6 has a role as an anti-inflammatory cytokine in the liver. Reperfusion injury can be attenuated by the administration of recombinant IL-6 and is aggravated in IL-6-deficient mice [53]. However, the clinical study shows that the lower concentration of IL-6, the higher graft survival rate, suggesting that IL-6 at reperfusion is a valid biomarker to predict long-term survival of graft [54]. Interestingly, IL-17 enhances the production of IL-6 and IL-8 in rheumatoid arthritis patient [55]. IL-17-mediated induction of IL-6 and IL-8 is transduced via activation of PI3K/Akt and NF-κB [55]. Thus, it is possible that reduction of IL-17 precedes the reduction of IL-6 produced in $CD11b^{+}$ infiltrated macrophages in the liver of PI3K $p110\gamma^{-/-}$ mice. IL-17 is expressed mainly in Th17 cells, subsets of γδ T cells and NK cells [56]. In addition, I evaluated the RORγt transcription factor by flow cytometer to assess whether these results were due to a decrease in Th17 cells. $ROR\gamma t^{+}$ T cell population did not change in PI3K $p110\gamma^{-/-}$ mice at 24 hours of reperfusion (Data not shown) although they are suggested to produce IL-17 [29]. These results demonstrated that the reduction of IL-17 was caused at the stage of cytokine production rather than at developmental stage of Th17 cells in

PI3K p110$\gamma^{-/-}$.

In conclusion, the current study is the first to document the role of PI3K p110γ in murine LIRI. I showed that LIRI was ameliorated by the reduction of pro-inflammatory cytokines such as IL-17 and the reduction of infiltrated macrophages into the damaged liver in PI3K p110$\gamma^{-/-}$ mice. This results suggest that PI3Kγ might be a suitable target for development of drugs that could specifically modulate the migration of macrophages and cytokine production in the liver.

References

[1] Huguet C, Gavelli A, Bona S. Hepatic resection with ischemia of the liver exceeding one hour. Journal of the American College of Surgeons. 1994;178:454-8.

[2] Liu DL, Jeppsson B, Hakansson CH, Odselius R. Multiple-system organ damage resulting from prolonged hepatic inflow interruption. Archives of surgery (Chicago, Ill : 1960). 1996;131:442-7.

[3] Lemasters JJ, Thurman RG. Reperfusion injury after liver preservation for transplantation. Annual review of pharmacology and toxicology. 1997;37:327-38.

[4] Vedder NB, Fouty BW, Winn RK, Harlan JM, Rice CL. Role of neutrophils in generalized reperfusion injury associated with resuscitation from shock. Surgery. 1989;106:509-16.

[5] Huguet C, Addario-Chieco P, Gavelli A, Arrigo E, Harb J, Clement RR. Technique of hepatic vascular exclusion for extensive liver resection. American journal of surgery. 1992;163:602-5.

[6] Delva E, Camus Y, Nordlinger B, Hannoun L, Parc R, Deriaz H, et al. Vascular

occlusions for liver resections. Operative management and tolerance to hepatic ischemia: 142 cases. Annals of surgery. 1989;209:211-8.

[7] Serracino-Inglott F, Habib NA, Mathie RT. Hepatic ischemia-reperfusion injury. The American Journal of Surgery.181:160-6.

[8] Henderson JM. Liver transplantation and rejection: an overview. Hepato-gastroenterology. 1999;46 Suppl 2:1482-4.

[9] Farmer DG, Amersi F, Kupiec-Weglinski J, Busuttil RW. Current status of ischemia and reperfusion injury in the liver. Transplantation Reviews. 2000;14:106-26.

[10] Jaeschke H, Farhood A. Neutrophil and Kupffer cell-induced oxidant stress and ischemia-reperfusion injury in rat liver. The American journal of physiology. 1991;260:G355-62.

[11] Bilzer M, Gerbes AL. Preservation injury of the liver: mechanisms and novel therapeutic strategies. Journal of hepatology. 2000;32:508-15.

[12] Jaeschke H. Role of reactive oxygen species in hepatic ischemia-reperfusion injury and preconditioning. Journal of investigative surgery : the official journal of the Academy of

Surgical Research. 2003;16:127-40.

[13] Rymsa B, Wang JF, de Groot H. O2-. release by activated Kupffer cells upon hypoxia-reoxygenation. The American journal of physiology. 1991;261:G602-7.

[14] Decker K. Biologically active products of stimulated liver macrophages (Kupffer cells). European Journal of Biochemistry. 1990;192:245-61.

[15] Ikarashi M, Nakashima H, Kinoshita M, Sato A, Nakashima M, Miyazaki H, et al. Distinct development and functions of resident and recruited liver Kupffer cells/macrophages. Journal of leukocyte biology. 2013;94:1325-36.

[16] Zigmond E, Varol C, Farache J, Elmaliah E, Satpathy AT, Friedlander G, et al. Ly6C hi monocytes in the inflamed colon give rise to proinflammatory effector cells and migratory antigen-presenting cells. Immunity. 2012;37:1076-90.

[17] Holt MP, Cheng L, Ju C. Identification and characterization of infiltrating macrophages in acetaminophen-induced liver injury. Journal of leukocyte biology. 2008;84:1410-21.

[18] Heymann F, Hammerich L, Storch D, Bartneck M, Huss S, Russeler V, et al. Hepatic macrophage migration and differentiation critical for liver fibrosis is mediated by the

chemokine receptor C-C motif chemokine receptor 8 in mice. Hepatology (Baltimore, Md). 2012;55:898-909.

[19] Zimmermann HW, Seidler S, Nattermann J, Gassler N, Hellerbrand C, Zernecke A, et al. Functional contribution of elevated circulating and hepatic non-classical CD14CD16 monocytes to inflammation and human liver fibrosis. PloS one. 2010;5:e11049.

[20] Hawkins PT, Anderson KE, Davidson K, Stephens LR. Signalling through Class I PI3Ks in mammalian cells. Biochemical Society transactions. 2006;34:647-62.

[21] Vanhaesebroeck B, Leevers SJ, Panayotou G, Waterfield MD. Phosphoinositide 3-kinases: a conserved family of signal transducers. Trends in biochemical sciences. 1997;22:267-72.

[22] Hirsch E, Katanaev VL, Garlanda C, Azzolino O, Pirola L, Silengo L, et al. Central role for G protein-coupled phosphoinositide 3-kinase gamma in inflammation. Science (New York, NY). 2000;287:1049-53.

[23] Kim N, Woo DC, Joo SJ, Song Y, Lee JJ, Woo CW, et al. Reduction in Renal Ischemia-Reperfusion Injury in Mice by a Phosphoinositide 3-Kinase p110gamma-Specific Inhibitor.

Transplantation. 2015;99:2070-6.

[24] Gao B, Jeong WI, Tian Z. Liver: An organ with predominant innate immunity. Hepatology (Baltimore, Md). 2008;47:729-36.

[25] Liu ZX, Han D, Gunawan B, Kaplowitz N. Neutrophil depletion protects against murine acetaminophen hepatotoxicity. Hepatology (Baltimore, Md). 2006;43:1220-30.

[26] Jaeschke H. Mechanisms of Liver Injury. II. Mechanisms of neutrophil-induced liver cell injury during hepatic ischemia-reperfusion and other acute inflammatory conditions. American journal of physiology Gastrointestinal and liver physiology. 2006;290:G1083-8.

[27] Selzner N, Selzner M, Odermatt B, Tian Y, Van Rooijen N, Clavien PA. ICAM-1 triggers liver regeneration through leukocyte recruitment and Kupffer cell-dependent release of TNF-alpha/IL-6 in mice. Gastroenterology. 2003;124:692-700.

[28] Wanner GA, Ertel W, Muller P, Hofer Y, Leiderer R, Menger MD, et al. Liver ischemia and reperfusion induces a systemic inflammatory response through Kupffer cell activation. Shock (Augusta, Ga). 1996;5:34-40.

[29] Eggenhofer E, Rovira J, Sabet-Baktach M, Groell A, Scherer MN, Dahlke M-H, et al.

Unconventional RORγt⁺ T Cells Drive Hepatic Ischemia Reperfusion Injury. The Journal of Immunology. 2013;191:480-7.

[30] Wu W-P, Tsai Y-G, Lin T-Y, Wu M-J, Lin C-Y. The attenuation of renal fibrosis by histone deacetylase inhibitors is associated with the plasticity of FOXP3(+)IL-17(+) T cells. BMC Nephrology. 2017;18:225.

[31] Liu T, Zhang Q, Mo W, Yu Q, Xu S, Li J, et al. The protective effects of shikonin on hepatic ischemia/reperfusion injury are mediated by the activation of the PI3K/Akt pathway. Scientific Reports. 2017;7:44785.

[32] Alatery A, Siddiqui S, Chan M, Kus A, Petrof EO, Basta S. Cross, but not direct, presentation of cell-associated virus antigens by spleen macrophages is influenced by their differentiation state. Immunology And Cell Biology. 2009;88:3.

[33] Čikoš Š, Bukovská A, Koppel J. Relative quantification of mRNA: comparison of methods currently used for real-time PCR data analysis. BMC Molecular Biology. 2007;8:113.

[34] Yue S, Zhou H, Wang X, Busuttil RW, Kupiec-Weglinski JW, Zhai Y. Prolonged

Ischemia Triggers Necrotic Depletion of Tissue-Resident Macrophages To Facilitate Inflammatory Immune Activation in Liver Ischemia Reperfusion Injury. Journal of immunology (Baltimore, Md : 1950). 2017;198:3588-95.

[35] De Henau O, Rausch M, Winkler D, Campesato LF, Liu C, Cymerman DH, et al. Overcoming resistance to checkpoint blockade therapy by targeting PI3Kgamma in myeloid cells. Nature. 2016;539:443-7.

[36] Chen GY, Nunez G. Sterile inflammation: sensing and reacting to damage. Nature reviews Immunology. 2010;10:826-37.

[37] Block H, Herter JM, Rossaint J, Stadtmann A, Kliche S, Lowell CA, et al. Crucial role of SLP-76 and ADAP for neutrophil recruitment in mouse kidney ischemia-reperfusion injury. J Exp Med. 2012;209:407-21.

[38] Nombela-Arrieta C, Lacalle RA, Montoya MC, Kunisaki Y, Megias D, Marques M, et al. Differential requirements for DOCK2 and phosphoinositide-3-kinase gamma during T and B lymphocyte homing. Immunity. 2004;21:429-41.

[39] Reif K, Okkenhaug K, Sasaki T, Penninger JM, Vanhaesebroeck B, Cyster JG. Cutting

edge: differential roles for phosphoinositide 3-kinases, p110gamma and p110delta, in lymphocyte chemotaxis and homing. Journal of immunology (Baltimore, Md : 1950). 2004;173:2236-40.

[40] Saudemont A, Garcon F, Yadi H, Roche-Molina M, Kim N, Segonds-Pichon A, et al. p110gamma and p110delta isoforms of phosphoinositide 3-kinase differentially regulate natural killer cell migration in health and disease. Proc Natl Acad Sci U S A. 2009;106:5795-800.

[41] Krenkel O, Tacke F. Liver macrophages in tissue homeostasis and disease. Nature Reviews Immunology. 2017;17:306.

[42] Jones GE, Prigmore E, Calvez R, Hogan C, Dunn GA, Hirsch E, et al. Requirement for PI 3-kinase gamma in macrophage migration to MCP-1 and CSF-1. Experimental cell research. 2003;290:120-31.

[43] Roberts AW, Lee BL, Deguine J, John S, Shlomchik MJ, Barton GM. Tissue-Resident Macrophages Are Locally Programmed for Silent Clearance of Apoptotic Cells. Immunity. 2017;47:913-27.e6.

[44] Scott CL, Zheng F, De Baetselier P, Martens L, Saeys Y, De Prijck S, et al. Bone marrow-derived monocytes give rise to self-renewing and fully differentiated Kupffer cells. Nature communications. 2016;7:10321.

[45] Lavin Y, Winter D, Blecher-Gonen R, David E, Keren-Shaul H, Merad M, et al. Tissue-resident macrophage enhancer landscapes are shaped by the local microenvironment. Cell. 2014;159:1312-26.

[46] Mantovani A, Sozzani S, Locati M, Allavena P, Sica A. Macrophage polarization: tumor-associated macrophages as a paradigm for polarized M2 mononuclear phagocytes. Trends in immunology. 2002;23:549-55.

[47] Hamilton TA, Zhao C, Pavicic PG, Datta S. Myeloid Colony-Stimulating Factors as Regulators of Macrophage Polarization. Frontiers in Immunology. 2014;5:554.

[48] Kaneda MM, Messer KS, Ralainirina N, Li H, Leem CJ, Gorjestani S, et al. PI3Kgamma is a molecular switch that controls immune suppression. Nature. 2016;539:437-42.

[49] Amano MT, Castoldi A, Andrade-Oliveira V, Latancia MT, Terra FF, Correa-Costa M, et

al. The lack of PI3Kgamma favors M1 macrophage polarization and does not prevent kidney diseases progression. International immunopharmacology. 2018;64:151-61.

[50] Tanaka T, Narazaki M, Kishimoto T. IL-6 in inflammation, immunity, and disease. Cold Spring Harb Perspect Biol. 2014;6:a016295.

[51] McCurry KR, Campbell DA, Jr., Scales WE, Warren JS, Remick DG. Tumor necrosis factor, interleukin 6, and the acute phase response following hepatic ischemia/reperfusion. The Journal of surgical research. 1993;55:49-54.

[52] Gabrilovich DI, Nagaraj S. Myeloid-derived suppressor cells as regulators of the immune system. Nature Reviews Immunology. 2009;9:162.

[53] Camargo CA, Jr., Madden JF, Gao W, Selvan RS, Clavien PA. Interleukin-6 protects liver against warm ischemia/reperfusion injury and promotes hepatocyte proliferation in the rodent. Hepatology (Baltimore, Md). 1997;26:1513-20.

[54] Faitot F, Besch C, Lebas B, Addeo P, Ellero B, Woehl-Jaegle ML, et al. Interleukin 6 at reperfusion: A potent predictor of hepatic and extrahepatic early complications after liver transplantation. Clinical transplantation. 2018;32:e13357.

[55] Hwang S-Y, Kim J-Y, Kim K-W, Park M-K, Moon Y, Kim W-U, et al. IL-17 induces production of IL-6 and IL-8 in rheumatoid arthritis synovial fibroblasts via NF-κB- and PI3-kinase/Akt-dependent pathways. Arthritis Res Ther. 2004;6:R120.

[56] Jin W, Dong C. IL-17 cytokines in immunity and inflammation. Emerg Microbes Infect. 2013;2:e60.

국문요약

배경: 조직 허혈 - 재관류 손상은 일반적으로 장기 또는 조직으로의 혈액 공급이 중단되고 재관류에 의한 혈액 순환을 재개할 때 발생하며, 급성 염증 반응이 유발된다. 따라서 허혈 - 재관류 손상 모델은 일반적으로 절제 수술 및 이식에 의한 급성 염증 반응의 비임상 모델로 사용된다. 이전의 연구에서 PI3K p110 감마의 약리적 억제가 신장 허혈 - 재관류 손상을 줄일 수 있음을 보여주었다. 따라서 이 연구는 간 허혈 - 재관류 손상에서 PI3K 감마의 역할에 대해 알기 위해 PI3K p110 감마 결핍 생쥐를 사용하여 실험을 진행하였다.

방법: 간문맥을 혈관 클램프로 집어 허혈 상태를 90 분간 유지하고 혈관 클램프를 제거하여 재관류를 시작함으로써 간 상부 70% 정도 부위에 허혈 – 재관류 손상을 유도하였다. 재관류 3 또는 24 시간후 생쥐를 희생시켰다. 간 손상은 혈청 ALT 수준과 조직학에 의해 평가하였다. 염증성 사이토카인 발현 수준은 qPCR에 의해 결정되었고, 각 사이토카인의 단백질 수준의 검출은 세포 내 염색을 수행하고 유세포 분석에 의해 분석하였다. 또한, 간 면역 세포 아군은 유세포분석에 의해 결정되었다.

결과: PI3K p110 감마 결핍 생쥐에서 간 허혈 – 재관류 손상이 감소하는 것을 혈청 ALT 수준과 조직병리학을 통해 확인하였다. PI3K p110 감마 결핍 생쥐의 간에서 야생형 생쥐와 다르게 염증 사이토카인 IL-6, IL-17 의 발현이 수술 후 3, 24 시간 후에 감소하는 것을 qPCR을 통해 발견하였다. 특히 허혈 3 시간 후 IL-6 와 IL-17 유전자 발현의 감소는 통계적으로 유의했다. 이러한 사이토카인을 생성하는 세포 종류를 규명하고 유전자 발현 양 감소를 단백질 수준에서 평가하기 위하여 세포내 염색을 통한 유세포분석을 실시한 결과, IL-6 를 발현하는 세포는 $CD11b^+$ 대식세포이고 IL-17 을 발현하는 세포는 T세포임을 알게되었다. 또한 PI3K p110 감마 결핍 생쥐의 간 면역세포 구성 중 전체 대식세포의 비율이 허혈 - 재관류 손상 이후 감소하였고, 특히 $CD11b^+$ $F4/80^+$ 한 손상된 조직으로 침윤된 대식세포의 비율이 유의하게 줄어들었다. 하지만 대식세포 M1 과 M2 분화에는 차이가 없었다.

결론: 이 실험결과들을 바탕으로 PI3K p110 감마가 생쥐에서 간 허혈 – 재관류 손상을 완화시키는 역할을 한다는 것을 확인할 수 있었고, 실험 결과를 종합하면 PI3K p110 감마 결핍은 염증성 사이토카인 발현의 감소와 간에서의 전체

대식세포의 비율을 감소시키고, 특히 염증성 조직으로 침윤된 대식세포의 비율을 감소시킴으로써 간 허혈 – 재관류 손상을 감소시키는 것으로 보인다.